Electronic structure of buried α-$FeSi_2$ and β-$FeSi_2$ layers: Soft-x-ray-emission and -absorption studies compared to band-structure calculations

S. Eisebitt,* J.-E. Rubensson, M. Nicodemus, T. Böske, S. Blügel, and W. Eberhardt
Institut für Festkörperforschung, Forschungszentrum Jülich, D-52425 Jülich, Germany

K. Radermacher and S. Mantl
Institut für Schicht- und Ionentechnik, Forschungszentrum Jülich, D-52425 Jülich, Germany

G. Bihlmayer
Institut für Physikalische Chemie, Universität Wien, A-1090, Wien, Austria
(Received 7 June 1994)

The electronic structure of buried α-$FeSi_2$ and β-$FeSi_2$ layers produced by ion-beam synthesis has been studied. Using fluorescence spectroscopies, we were able to investigate the silicide layers, which are buried below a 600 Å Si cap layer, *in situ*. The occupied local Fe d density of states was determined by Fe L_3 soft-x-ray-emission spectra, excited both with high-energy electrons and monochromatized synchrotron radiation. Using soft-x-ray-absorption spectra recorded in the fluorescence-yield mode at the same Fe L_3 edge, the unoccupied Fe d density of states was determined. The formation of a band gap of 0.8 ± 0.2 eV in the electronic states of d symmetry at the Fe atoms of β-$FeSi_2$ could be observed in the experiments. We present *ab initio* band-structure calculations for α-$FeSi_2$ and β-$FeSi_2$ and compare the results to the spectroscopic data. The influence of a core hole on the soft-x-ray-absorption spectrum is studied by calculating the electronic structure of a substitutional impurity in the form of a core $2p_{3/2}$ ionized Fe atom using a supercell calculation.

I. INTRODUCTION

Transition metal silicides have been studied intensively in the last decade for a variety of reasons. One driving force is their potential for application in very large scale integration and for the design of fast elements within microelectronic device technology.[1–3] This potential originates from the electronic properties of the silicides in conjunction with the possibility for epitaxial growth in and on Si.

While most of the silicides studied so far are metallic and thus interesting for the production of connections and high-quality Schottky barriers to Si, β-$FeSi_2$ has recently attracted interest because it is a semiconductor.

$FeSi_2$ exists in two thermodynamically stable (bulk) phases, as tetragonal, metallic α-$FeSi_2$ and as orthorhombic, semiconducting β-$FeSi_2$.[4,5] The phase transition temperature is $\approx$ 937 °C,[6] where β-$FeSi_2$ is the low-temperature stable phase. β-$FeSi_2$ has an indirect band gap of about 0.78 eV,[7,8] and a slightly larger direct gap of about 0.83 eV.[7–14]

The formation of the band gap in β-$FeSi_2$ has been described in terms of a Jahn-Teller-like transition from a metallic $FeSi_2$ phase in a hypothetical CaF_2 structure to the orthorhombic β phase.[15] The presence of the α and β phases with a metallic to semiconducting transition makes $FeSi_2$ an interesting system for basic studies of the electronic structure.

Ion-beam synthesis (IBS) has overcome growth problems for a variety of transition metal silicides.[16] In particular, well-defined layers of α- and β-$FeSi_2$ buried in Si can be produced by this technique.[17,18]

Conventional electron spectroscopies are not suited to studying the electronic structure in these buried layers due to the short electron mean free path. However, photon-in–photon-out spectroscopies can be used to extract physical information from buried structures. We have studied buried layers of α-$FeSi_2$ and β-$FeSi_2$ synthesized by IBS using fluorescence-yield (FY) soft-x-ray-absorption (FY-SXA) and soft-x-ray-emission (SXE) spectroscopy. In SXA, a core electron is promoted to an unoccupied electronic state. The absorption as a function of photon energy can be monitored by the FY produced by the radiative decay of the core hole. In SXE, a previously prepared core hole is filled by a valence electron in a radiative process. The generated fluorescence radiation is analyzed in a spectrometer. As we will show in Sec. IV B, the interpretation of SXE and SXA spectra can often be simplified. In such a case the SXA (SXE) spectra become a direct measure of the unoccupied (occupied) density of states (DOS). As in both cases a localized core orbital at a specific atomic species is involved in the transition, the *local* DOS at these sites is monitored. Due to dipole selection rules, only valence states of certain angular momentum are probed (*partial* DOS). Hence, SXE and SXA yield information about the local partial DOS (LPDOS). In order to probe the Fe d states, which are important for the electronic structure in $FeSi_2$ as a $3d$ transition metal compound, we have measured the Fe L absorption and emission spectra. Combining both techniques, we

0163-1829/94/50(24)/18330(11)/$06.00

get a complete experimental picture of the Fe d DOS in α-$FeSi_2$ and β-$FeSi_2$.

From SXE data on as-implanted (i.e., not annealed) samples we obtain information about the IBS process.

The experimental results are complemented by *ab initio* band-structure calculations for both phases of $FeSi_2$. While the electronic structure of β-$FeSi_2$ has been calculated before by several groups,[15,19] we are not aware of any previous calculation of α-$FeSi_2$. The band-structure results such as the calculated and then broadened occupied Fe d DOS of the silicides can be compared directly to the SXE spectra. A comparison with the SXA spectra is more involved: according to the final state rule,[20] the observed spectra should reflect the LPDOS of the silicides *in presence of a core hole.* Therefore we calculate in addition both silicides with a core electron transferred to the valence electrons and compare the broadened unoccupied Fe d DOS of these calculations with SXA data. The presence of a core hole in the calculation leads to a good quantitative and qualitative understanding of the experimental SXA results.

This publication is organized as follows. The techniques used in the experiments and those used in the band-structure calculations are presented in Secs. II and III, respectively. Results for α-$FeSi_2$ and β-$FeSi_2$ are presented and discussed in Sec. IV. First, the theoretical results are treated (IV A), and then the kind of information that can be obtained experimentally by the spectroscopies used is discussed (IV B). Experimental results concerning the occupied electronic states (IV C) and the unoccupied electronic states (IV D) are presented and compared to the theoretical results. Finally the SXE spectrum of an IBS sample in the unannealed, as-implanted state (IV E) is discussed.

II. EXPERIMENTAL TECHNIQUES

Buried layers of $FeSi_2$ were produced by IBS.[17] After implanting 2.8×10^{17} $Fe^+\,cm^{-2}$ at 200 kV into a (111)Si wafer at 350 °C (as-implanted samples), rapid thermal annealing at 1150 °C for 10 s led to an α-$FeSi_2$ layer of 125 nm thickness, covered by a 60 nm Si cap layer. On other samples prepared following exactly the same procedure, composition, interface quality, and the overall geometry of the layers were checked by Rutherford backscattering spectroscopy (RBS) and cross-sectional transmission electron spectroscopy (TEM). X-ray-diffraction (XRD) measurements indicated the presence of α-$FeSi_2$ only.

By furnace annealing at 800 °C (i.e., below the phase transition temperature) for 17 h the α-$FeSi_2$ layers were converted into β-$FeSi_2$. Again, the samples were characterized by XRD, RBS, and TEM.[17]

SXE spectra were recorded in a new spherical grating grazing incidence Rowland spectrometer, which will be described in detail elsewhere.[21] Electrons with 4.7 keV energy and monochromatized synchrotron radiation from the X1B monochomator[22] at the National Synchrotron Light Source (NSLS) were used for excitation. The best resolution in the emission spectra, 0.4 eV, was achieved in second order on a 5 m grating with 1200 lines/mm using a 10 μm entrance slit.

FY-SXA spectra were recorded using the SX-700-II monochromator[23] at the Berliner Elektronenspeicherring Gesellschaft für Synchrotronstrahlung GmbH (BESSY) with a resolution of 1.0 eV at the Fe L edge. Absorption was measured by the partial fluorescence yield using a Ge detector with a resolution of 100 eV in a near-normal incidence and grazing take off setup in which saturation was found to be negligible.[24]

III. DETAILS OF THE ELECTRONIC STRUCTURE CALCULATIONS

The calculations are based on the density functional theory in the local density approximation (LDA). For the exchange and correlation potential we used the Hedin-Lundqvist parametrization.[25] The density functional equations are solved by applying the the full-potential linearized augmented plane wave (FLAPW) method,[26] which is known to be precise for open structures and transition metals. The eigenstates of the core electrons (Fe: [Ar], Si: [Ne]) are obtained as solutions of the Dirac equation and for the valence electrons we used a scalar relativistic approach. The crystal structure of α-$FeSi_2$ is tetragonal with three atoms in the unit cell. β-$FeSi_2$ has 48 atoms in a base-centered orthorhombic unit cell. This unit cell contains two inequivalent Fe sites with eight atoms of Fe(1) type and eight atoms of Fe(2) type as well as two inequivalent Si sites with 16 atoms for each type. Since the electronic structures of the two different Fe and Si atoms are rather similar we discuss below always the average of the Fe and Si atoms and compare these with the experimental data. The Bravais matrices and the positions of the atoms can be found in Ref. 5. Basis sets of approximately 90 augmented plane waves (APW) per atom gave sufficiently accurate results for all calculated quantities. This was checked against a 180 APW/atom calculation of α-$FeSi_2$. Self-consistent calculations were carried out with 120 **k** points in the irreducible wedge of the Brillouin zone of α-$FeSi_2$ and 15 **k** points in the irreducible wedge of β-$FeSi_2$. The DOS of β-$FeSi_2$ was calculated with an increased number of 60 **k** points.

For the theoretical studies of the silicides with core hole the complete final state screening effects are treated by calculating the electronic structure of a substitutional impurity in the form of a core-ionized impurity imbedded in a supercell. The core hole to be screened is taken as a Fe $2p_{3/2}$ state since this corresponds to the transition measured in the experiment. The Fe core electron was transferred to the valence band (α-$FeSi_2$) or conduction band (β-$FeSi_2$) of the silicides. For α-$FeSi_2$ the calculations were performed using a 24-atom supercell with one core hole and for β-$FeSi_2$ the simple unit cell of β-$FeSi_2$ with two core holes in one layer of Fe(1) was used. Thus a minimal distance of $\sim$ 10 a.u. between two holes is ensured. This was found sufficient to avoid a significant hole-hole interaction. As before for β-$FeSi_2$, we used for both supercells 15 **k** points to obtain a self-consistent electronic structure and 60 **k** points for the DOS calculation.

IV. RESULTS AND DISCUSSION

A. Band-structure calculations

From the calculated DOS of α-$FeSi_2$ (Fig. 1) we can derive a simple picture of the bonding properties of these silicides. The Si s band is located between -13 and -7 eV (relative to the Fermi energy E_F). Between -7 and -2 eV the four Si p electrons overlap with the six Fe d electrons of t_{2g} type, thus forming strong bonding orbitals in the Fe-Si direction. The two remaining Fe-d (e_g-type) orbitals are located above and below E_F. Pointing in the Fe-Fe direction, they are of nonbonding character. The peak in the DOS between -1.5 eV and E_F contains electrons of Fe d and some Si p type; the other peak is located between E_F and 1.5 eV and consists of Fe d DOS. Above the minimum at 1.5 eV a mixture of Fe d and Si s, p and d states dominates the DOS.

The band structure of α-$FeSi_2$ (Fig. 2) confirms this picture. The flat d bands above and below E_F are sparsely connected. In β-$FeSi_2$ these small connections break and a gap opens between the two Fe e_g-type states (Fig. 3). The calculated band gap of 0.78 eV is in fair agreement with experimental data.[7,8] Christensen[15] has suggested that the LDA could give correct results for band gaps that are opened by a Jahn-Teller-like effect. From the calculation the band gap of β-$FeSi_2$ is almost direct and a slightly larger direct gap (0.82 eV) at the Y point can be seen in the band structure in Fig. 4. Comparing with Refs. 15 and 19 one has to take into account that in a simple orthorhombic setup the Γ and Y points coincide, and only one maximum in the valence bands can be seen. As the Γ-Z direction is perpendicular to the basis of the lattice, the gap is located at $\frac{1}{2}(\Gamma\text{-}Z)$ in both cases. The electron states at $\frac{1}{2}(\Gamma\text{-}Z)$ and Y are of mixed Fe d, p and Si p type while the holes are of pure Fe d character. This is consistent with the results of Eppenga,[19] who also calculated the transition probabilities between both states and found them to be quite small.

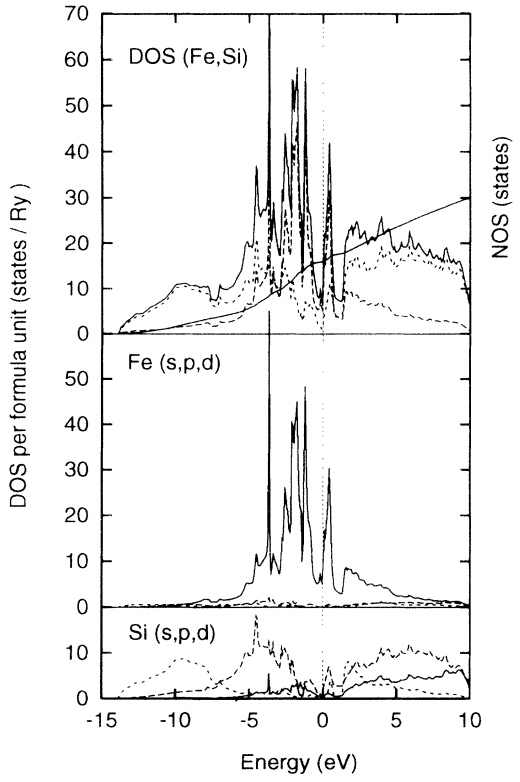

FIG. 1. Density of states (DOS) of α-$FeSi_2$. Top panel shows the total DOS (full line) decomposed into the local (L)DOS of Fe (long dashed line) and Si (short dashed line). The middle and bottom panel show the LDOS's of Fe and Si, respectively, decomposed into angular momentum contributions s (short dashed line), p (long dashed line), and d (full line). For Fe the s and p DOS's are insignificant compared to d contributions. The top panel contains also the number of states (NOS) (full line, same scale). DOS and NOS are expressed in units of electrons/Ry per formula unit (f.u.) and electrons/f.u., respectively. Fermi energy is indicated by a vertical dotted line at 0 eV.

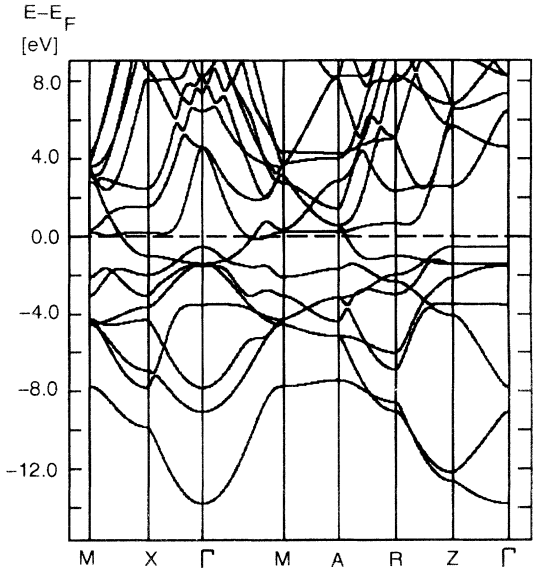

FIG. 2. Band structure of α-$FeSi_2$ along symmetry lines in the first Brillouin zone. The position of the Fermi energy is indicated by a horizontal dashed line at 0 eV. The notation of the high-symmetry points was chosen according to Bradley and Cracknell (Ref. 44).

Total energy calculations for both silicides at experimental lattice constants correctly predict that β-$FeSi_2$ is indeed more stable than α-$FeSi_2$, but the energy difference between the phases is small (1.7 mRy/atom).

To compare with the SXA experiments, we also calculated both phases with an Fe $2p_{3/2}$ core hole (Fig. 5). In these calculations, care has to be taken to screen the core holes so that no "multiple-hole" effects arise. A hole-hole spacing of approximately 10 a.u. was found to be appropriate for these structures.

In α-$FeSi_2$ a small peak just below E_F arises, consisting of Fe d DOS, mostly from the Fe with the core hole, and Si p states. The peak above E_F in ordinary α-$FeSi_2$ is sharpened in the structure with the core hole and a

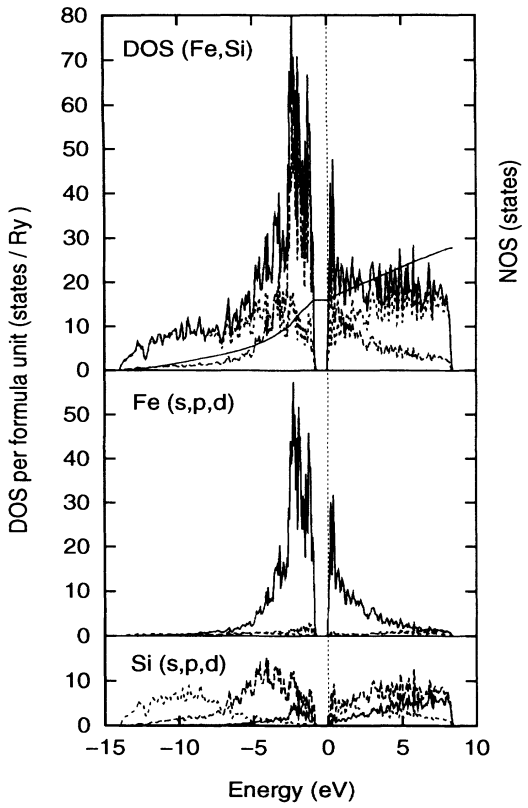

FIG. 3. Density of states (DOS) of β-$FeSi_2$, using the same notation as Fig. 1. The local densities of states of Fe and Si are the average over the two inequivalent Fe and Si sites, repectively, in the unit cell of β-$FeSi_2$.

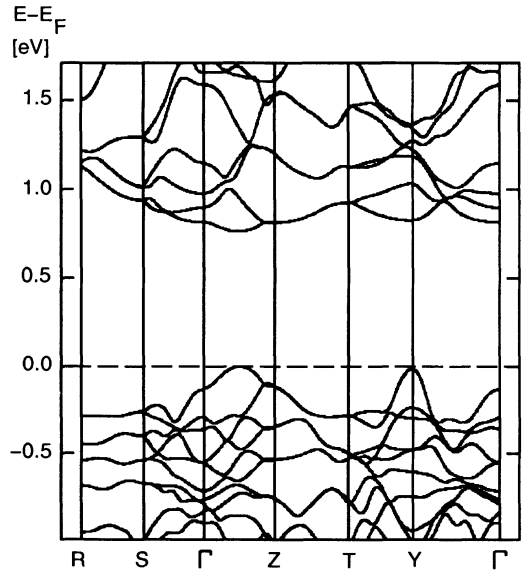

FIG. 4. Band structure of β-$FeSi_2$ along symmetry lines in the first Brillouin zone and for energies close to the band gap. The position of the Fermi energy indicated by a horizontal dashed line at 0 eV is somewhere in the band gap and is arbitrarily positioned at the top of the valence band. The notation follows Ref. 44.

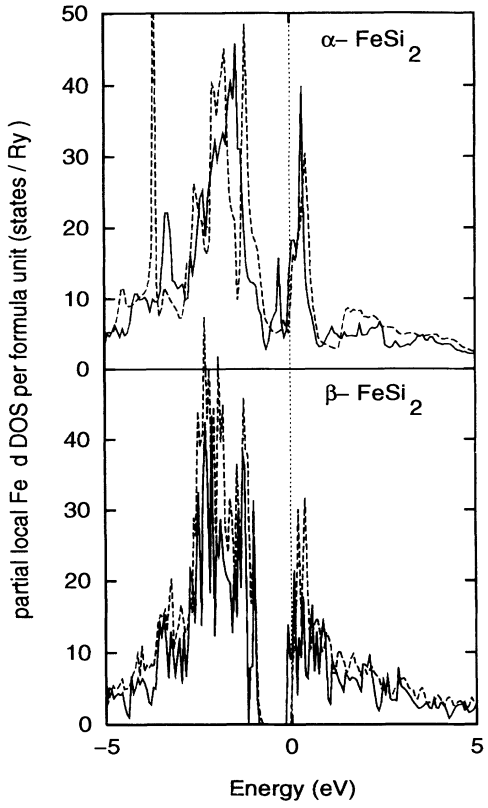

FIG. 5. Local partial density of states (LPDOS) of Fe d electrons in α-$FeSi_2$ (top panel) and in β-$FeSi_2$ (lower panel). Compared are the DOS's of Fe atoms with a $2p_{3/2}$ core hole (full line) and without one (dashed line). LPDOS of the atom without core hole is expressed in units of electrons/Ry per formula unit. For better comparison the LPDOS of the atom with core hole is scaled in magnitude to have the same formula unit as the one without core hole. In β-$FeSi_2$ the core hole was introduced in one layer of Fe(1) and the LPDOS of the Fe atoms without core hole is the average over the remaining Fe(1) and Fe(2) type atoms. The Fermi energy is indicated by a vertical dotted line at 0 eV.

shoulder on the low-energy side appears. This shoulder is also visible in the SXA spectra. Above 1.4 eV the DOS is not changed by the core hole.

In β-$FeSi_2$ the calculation shows the valence band to be almost unaffected by the core hole. The large double peak at the bottom of the conduction band is split into four smaller ones and one of these peaks is occupied by the excited core electron. Again this peak consists of Fe d and Si p states; most of the Fe d DOS is contributed from the Fe with the core hole. At the end of the Fe "e_g" band (1.0 eV), no significant influence on the DOS can be detected.

The band structure of β-$FeSi_2$ with the core hole (Fig. 6) gives a more detailed account of these observations. The highest valence band maximum is still between the Γ and Z points of the Brillouin zone and there is a second maximum at the Y point. Due to the introduction of core holes the symmetry is reduced and the degeneracy of certain bands along high symmetry lines is

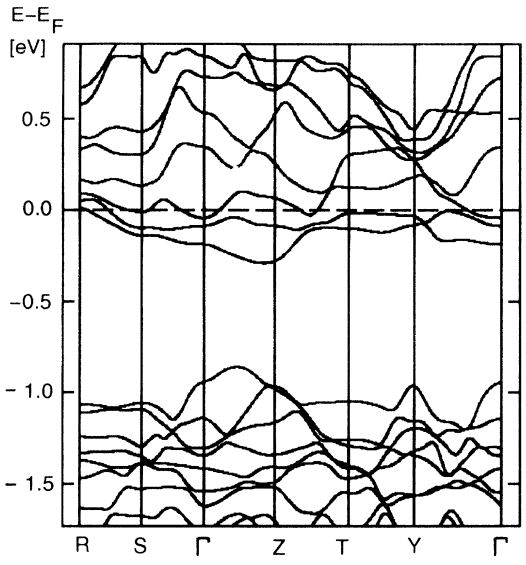

FIG. 6. Band structure of β-$FeSi_2$ including an Fe $2p_{3/2}$ core hole for 2 Fe atoms in the unit cell of 24 atoms. The band structure is shown along symmetry lines in the first Brillouin zone and for energies close to the band gap. The position of the Fermi energy is indicated by a horizontal dashed line at 0 eV.

lifted. This is particularly drastic for conduction bands. This explains the split of the double peak observed in Fig. 5 into four smaller ones. In particular the conduction band minimum does not coincide in **k** space anymore with the valence band maximum.

B. DOS information from soft-x-ray spectra

The spectral shape observed in SXE or SXA spectroscopy is related to the occupied (SXE) and unoccupied (SXA) LPDOS of the material investigated. Often electron correlation and dynamical effects can be neglected; then the observed intensity I_p in transition involving a photon of energy $\hbar\omega$ to or from a core level of p symmetry is[27]

$$I_p \propto (\hbar\omega)^3[N_s(E)M^2_{p,s}(E) + \tfrac{2}{5}N_d(E)M^2_{p,d}(E)]. \quad (1)$$

Here N_s and N_d denote the DOS of s or d character locally at the atomic species involved in the transition. For $3d$ transition metals $M^2_{p,d}(E) \gg M^2_{p,s}$, so that the influence of the Fe s DOS is small compared to that of the Fe d DOS. The matrix elements $M_{p,i}(E)$ vary slowly over the narrow energy interval of interest[28] without adding fine structure to the observed spectra. The factor $(\hbar\omega)^3$ is present in SXE only, due to the cubic energy dependence of the density of states for photons. (SXA spectra are normalized to the incident photon flux.) Another difference between SXE and SXA is that according to the final state rule[20] the measured DOS in SXA is the DOS with a core hole present. The impact of this core hole on the LPDOS depends on the material investigated. We will come back to this point when discussing the SXA spectra in comparison with the band-structure calculations.

Inherent broadening results from the finite lifetimes of the initial and final states. We expect the core hole lifetime width to be close to the value for elemental Fe, 0.24 eV.[29] The lifetime of the excited electron in SXA and the valence hole in SXE varies from negligible at the Fermi level (E_F) to 1–2 eV for energies deeper in the corresponding bands, resulting in an extra broadening at the corresponding transition energies.

In general the spectra can be affected by correlation and dynamical effects. In strongly correlated systems, which are characterized by very narrow bands, SXE and SXA cannot be interpreted in the one-electron picture leading to the DOS approach described above. A description in terms of quasiatomic excitations is then more appropriate.[31] As the d band in α-$FeSi_2$ and β-$FeSi_2$ is spread out due to the interaction of Fe d and Si p states, we expect correlation effects to be small. If correlation is important at all, we expect it to occur in the narrow e_g-type states around E_F (between -1.5 eV and 1.5 eV in the calculations). We will further investigate this possibility in the context of the SXE spectra.

Dynamical effects can introduce additional structure in free-electron-like systems, which are characterized by very broad bands.[32,33] Due to the presence of the narrow e_g-type states in addition to the low DOS at the Fermi level we expect these effects to be negligible in α- and β-$FeSi_2$.

C. Occupied Fe *d* DOS

In Fig. 7 we compare results from the band-structure calculation to the SXE spectra excited with 4.7 keV electrons of α-$FeSi_2$ and β-$FeSi_2$. Circles represent the experimental data, while the solid lines show the results of the calculations. The calculation has been broadened with a Lorentzian of 0.24 eV full width at half maximum (FWHM) to account for the core hole lifetime broadening, with an energy-dependent Lorentzian of $0.03(E - E_F)^2$ eV to account for the lifetime of the valence hole in the final state of the SXE process, and with a Gaussian of 0.4 eV FWHM to account for the experimental resolution. To establish the energy scale, the Fermi level was defined as the energy corresponding to a 50% intensity drop in the high-energy flank of the SXE spectrum of metallic α-$FeSi_2$.

The dominating peak at about -1.3 eV in both spectra can be attributed to the nonbonding, e_g-type Fe d states. Experiment and theory agree well in the position and the shape of the Fe d LPDOS. Even though it is not possible to compare experiment and theory on an absolute energy scale, the experimental spectra of α-$FeSi_2$ and β-$FeSi_2$ are carefully calibrated relative to each other and so are the calculated spectra. As can be seen in Fig. 7, the relative peak positions between the α-$FeSi_2$ and the β-$FeSi_2$ spectrum are reproduced by the calculation. The overall agreement indicates that the simple LPDOS model for the SXE process is valid in the present case. Furthermore, the shape of the spectra is predicted well by the calculation. The shape of this peak is asymmetric in both spectra, containing a low-energy tail below -2 eV. We interpret this tail as due to bonding Fe d states involved

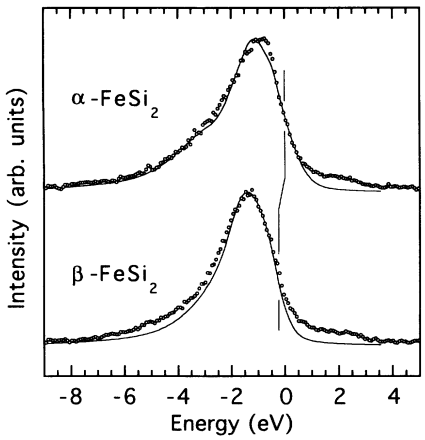

FIG. 7. SXE spectra (circles) recorded with an experimental resolution of 0.4 eV for buried layers of α-$FeSi_2$ (top) and β-$FeSi_2$ (bottom) are shown and referred to the Fermi energy. The underlying curves are the Fe d LPDOS's of our band-structure calculation (Figs. 1 and 3) broadened in order to account for the lifetime of the core hole (Lorentzian 0.24 eV FWHM) and the valence hole [Lorenzian $(E - E_F)^2$0.03 eV FWHM] and the experimental resolution (Gaussian 0.4 eV). The energy scales of the experimental and theoretical curves are shifted relative to each other by 0.6 eV for easier comparison (theory shifted to higher energy). Markers refer to the SXE spectra and indicate the 0.24 eV shift of the high-energy flank in the two spectra.

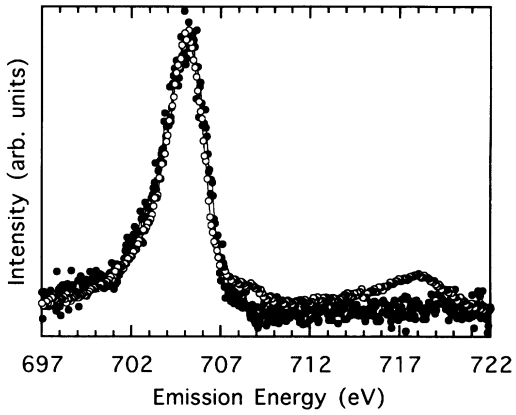

FIG. 8. SXE spectra for β-$FeSi_2$, excited with 4.7 keV electrons (open circles) and photons of 710 eV energy (filled circles). Smoothed lines have been drawn through the data points to guide the eye. The photon-excited spectrum was recorded with slightly lower resolution than the electron-excited spectrum. Due to the low excitation energy in the former case, the L_2 emission (around 718 eV) and the double-hole satellites (between about 707 eV and 710 eV) are suppressed.

in the Si p–Fe d bonds. This interpretation is supported by peaks of the LPDOS at corresponding energies in the band structure calculation.

The calculation predicts a shoulder due to these bonding states at about -3 eV in the Fe d DOS of α-$FeSi_2$ while for β-$FeSi_2$ only a low-energy tailing of the main peak is predicted as the structure related to the corresponding bonding states is closer in energy to the main peak. Additional experimental confirmation for this interpretation is given by the spacing of 1.6 eV observed between Fe d and Si p–Fe d related structures in Si SXE spectra of $FeSi_2$,[30] and by analogous results in a previous SXE investigation of $CoSi_2$.[34]

We note that the α-$FeSi_2$ spectrum is somewhat broader (FWHM = 2.7 eV) than the β-$FeSi_2$ spectrum (FWHM = 2.6 eV). Based on the calculations we attribute this difference partly to the difference in the bonding states.

In the high-energy region above E_F between about 0.5 eV and 3.5 eV, we observe a satellite which can be attributed to additional valence excitations created by the 4.7 keV electrons used to produce the core hole for SXE. For energy reasons this satellite cannot be a normal DOS feature. In Fig. 8, we present a SXE spectrum for β-$FeSi_2$ excited with photons of 710 eV energy (with a FWHM of about 4 eV). As the photon energy was tuned to be close above the Fe $2p_{3/2}$ binding energy in $FeSi_2$, double-excitation satellites (and Fe L_β emission) should be suppressed.[35] The spectrum was recorded with slightly lower resolution than the electron-excited spectrum, resulting in the larger width of the main peak. A clear reduction of intensity between about 707 eV and 710 eV is seen, corresponding to the same high-energy region above E_F mentioned above. This reduction confirms that the intensity in the electron-excited spectrum in this region is due to double excitations. The presence of this satellite is a direct indication of correlation in β-$FeSi_2$, showing that an additional valence hole is not fully screened during the core hole lifetime. Apart from this satellite all the spectra shown here are independent of the means of excitation, supporting their interpretation in terms of the LPDOS in a single-electron picture.

SXE spectra for β-$FeSi_2$, α-$FeSi_2$, an as-implanted sample (ai), and elemental Fe are shown in Fig. 9. The spectra were calibrated using the literature value for the Fe L_3 emission line, 705.0 eV,[36] and its separation from the L_2 line as deduced from the Fe $L_{2,3}$ spin-orbit splitting.[37] All spectra are dominated by the Fe d states, giving rise to the peak at around 705.0 eV. While this peak is symmetric in Fe, it has a low-energy tail in both silicide phases and in the as-implanted sample, indicating the splitting of the bonding states and the nonbonding states as discussed before.

Going from the metal to the silicides, the peak narrows: FWHM Fe (3.5 eV) > FWHM ai (3.2 eV) > FWHM α (2.7 eV) > FWHM β (2.6 eV). The bandwidth in Fe is solely determined by the Fe d–Fe d interaction. This interaction is reduced in the silicides due to the increased Fe-Fe distances and the reduced number of nearest Fe neighbors.[5] The narrowing going from Fe metal to the as-implanted sample already indicates silicide formation, and the further narrowing due to the heat treatment indicates the presence of more than one phase in the as-implanted sample. The difference in width between α- and β-$FeSi_2$ is in line with the fact that the average Fe-

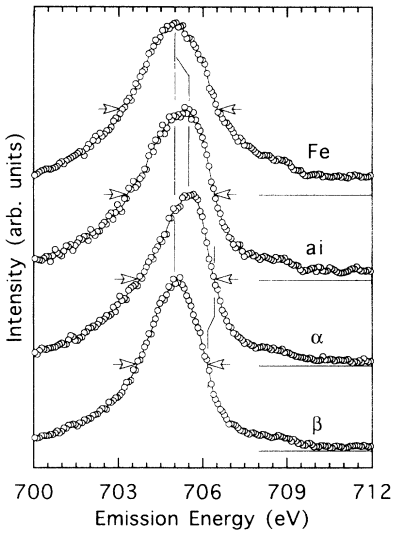

FIG. 9. SXE spectra for Fe, an as-implanted sample (ai), α-$FeSi_2$, and β-$FeSi_2$, excited with 4.7 keV electrons and recorded with 0.4 eV resolution. The smoothed lines through the data points are meant as a guide to the eye. The 0.24 eV shift between the high-energy flanks of the α-$FeSi_2$ and β-$FeSi_2$ SXE spectra is indicated by a marker.

Fe distance is somewhat larger in β-$FeSi_2$. The calculations, however, do not support this simple picture, but attribute the difference to a larger energy spacing between nonbonding and bonding states in α-$FeSi_2$.

The centroid of the peak in the α-$FeSi_2$ SXE spectrum is shifted by 0.5 eV towards higher energy compared to the spectra of β-$FeSi_2$ and Fe, which peak at the same energy.

The Fermi level cannot be directly determined from a spectral feature in the α-$FeSi_2$ SXE spectrum due to the contribution of satellite intensity to the spectrum in this region. However, this contribution is small (as discussed above) and of the same amount for α-$FeSi_2$ and β-$FeSi_2$. The energy shift in the high-energy flank of the spectra was determined by comparing the energies corresponding to a 50% intensity drop in the flank. The high-energy flank in the spectrum of the β phase is located 0.24 eV below the corresponding structure in the α-$FeSi_2$ spectrum.

We attribute this shift and the peak shifts described above to a changed shape of the DOS, reflecting the opening of the gap in the transition from the metallic α to the semiconducting β phase of $FeSi_2$. The opening of this gap occurs within the electronic states of d symmetry at the Fe sites and can thus be seen in the valence band $\rightarrow$ Fe $2p_{3/2}$ SXE process due to its selectivity with respect to the atomic species and the angular momentum. We will discuss the gap in more detail in conjunction with the additional information on the unoccupied states in Sec. IV D.

In x-ray photoelectron spectroscopy (XPS),[38,39] the Fe $2p_{3/2}$ core level in $FeSi_2$ was found to be shifted by 0.4 eV towards higher binding energy relative to Fe. This core level shift contributes to the observed shift of the silicides relative to Fe. However, as far as the 0.24 eV shift *between* the SXE of α-$FeSi_2$ and β-$FeSi_2$ is concerned, we expect the influence of chemical shifts to be negligible in comparison to the influence of the DOS, as the chemical environment of the Fe atoms is very similar in both phases.

D. Unoccupied Fe *d* DOS

In Fig. 10 we compare the FY-SXA spectra of buried β-$FeSi_2$ and α-$FeSi_2$ layers (circles) to the unoccupied part of the Fe d DOS from our band-structure calculation of both $FeSi_2$ phases (line). The calculations include the presence of the $2p_{3/2}$ core hole at the Fe site in the SXA process as described in Sec. III. They were broadened to account for the lifetime of the core hole and the excited electron with Lorentzians of 0.24 eV FWHM and $0.03(E-E_F)^2$ eV FWHM, respectively, and a Gaussian of 1.0 eV to account for the experimental resolution.

The SXA spectra were referred to the Fermi energy scale taking the energy correponding to a 50% intensity rise in the absorption edge of the α-$FeSi_2$ spectrum as the origin on the Fermi energy scale. The actual transition energies in the SXA experiment are 706.6 eV higher.

Above the Fe L_3 absorption threshold a broad peak is observed in both experimental spectra, generated by transitions from the Fe $2p_{3/2}$ level into the conduction

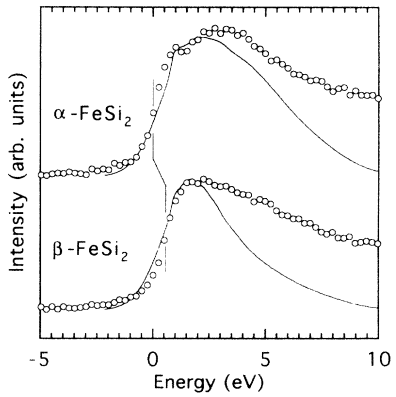

FIG. 10. FY-SXA spectra (circles) for buried layers of α-$FeSi_2$ (top) and β-$FeSi_2$ (bottom) recorded at the Fe L_3 absorption edge are shown. All spectra are recorded with a resolution of 1.0 eV in partial fluorescence-yield mode. The 0.45 eV shift between the low-energy flanks of the α-$FeSi_2$ and β-$FeSi_2$ FY-SXA spectra is indicated by markers. The experimental Fermi energy scale is shown at the bottom of the figure. The underlying lines show the results of the band-structure calculation for α-$FeSi_2$ and β-$FeSi_2$ (Figs. 1 and 3). They have been shifted up by 0.8 eV for easier comparison to the experiment. The potential of an Fe $2p_{3/2}$ core hole as present in the SXA process was included in the calculation in a supercell approach. The calculated Fe d LPDOS's were broadened in order to account for the lifetime of the core hole (Lorentzian 0.24 eV FWHM) and the valence electron [Lorenzian $(E-E_F)^2 0.03$ eV FWHM] and the experimental resolution (Gaussian 1.0 eV).

band. The shape of the spectra is very similar to recently published Fe L_3 absorption spectra of α-$FeSi_2$ and β-$FeSi_2$, recorded in the total-electron-yield mode.[40] Though the overall shape of both SXA spectra is similar, distinct differences in the fine structure can be seen. In α-$FeSi_2$ a shoulder at 1 eV appears in addition to the main peak at 3 eV, while in β-$FeSi_2$ the main peak is located at 2 eV and no low-energy shoulder can be observed. The absorption edge in the semiconducting β phase was found to be shifted by 0.56 eV towards higher energy compared to the metallic α phase.

We attribute the low-energy shoulder in the α-$FeSi_2$ spectrum to the contribution of unoccupied nonbonding Fe d states just above the Fermi energy, appearing as a shoulder in SXA due to the Fermi cutoff. Our calculation (Fig. 5) supports this interpretation, showing a region of high Fe d DOS at E_F. Hence, the Fermi level in α-$FeSi_2$ is located in the high-energy region of the nonbonding states. This interpretation is in agreement with previous results for $CoSi_2$, where a corresponding shoulder could be related to the nonbonding states as well.[34]

In contrast to the α-$FeSi_2$ spectrum, no shoulder close to E_F can be seen in the spectrum of β-$FeSi_2$. This is a consequence of the semiconducting character of β-$FeSi_2$. Here, the Fermi energy is located in the gap that opens within the nonbonding states and there is no particularly sharp Fe d DOS feature close to E_F.

Though the calculations describe the main features correctly, the calculated Fe d DOS in the high-energy region of both spectra is significantly lower than the corresponding SXA spectra. We do not have a conclusive explanation for this observation. However, the same kind of discrepancy in the high-energy region between calculated LPDOS and SXA spectra has been observed before.[41,42]

We would like to emphasize the importance of the inclusion of the core hole effects into the band-structure calculation in order to compare to the SXA data. As can be seen from the broadened DOS curves shown in Fig. 11, the agreement of the band-structure calculation with the SXA experiment is considerably improved for α-$FeSi_2$ when the core hole is taken into account. This finding supports the final state rule[20] for the SXA process.

It is known for simple metallic systems that the additional core hole potential shifts spectral weight within the unoccupied DOS towards lower energies. For transition metal silicides in particular it was found that a core hole at a Si site shifts spectral weight within the unoccupied states towards lower energies.[41]

At first glance this appears not to be true for the Fe d DOS in α-$FeSi_2$ and β-$FeSi_2$. While the relative spectral weight of the spectrum, i.e., the shape, is not altered in β-$FeSi_2$, the calculated DOS including the core hole fits the experimental spectrum of α-$FeSi_2$ better because the shoulder close to E_F is *reduced* in intensity while the peak at about 1.2 eV and the adjacent region up to 7 eV seem to be intensified upon inclusion of the core hole in the calculation (see Figs. 10 and 11). This effect, however, is due to the specific shape of the Fe d DOS of α-$FeSi_2$. In particular, the sharp and intense DOS feature around E_F (between -0.1 eV and 0.7 eV in the calculation) in conjunction with the adjacent low DOS region (above 0.7 eV) is responsible for this behavior.

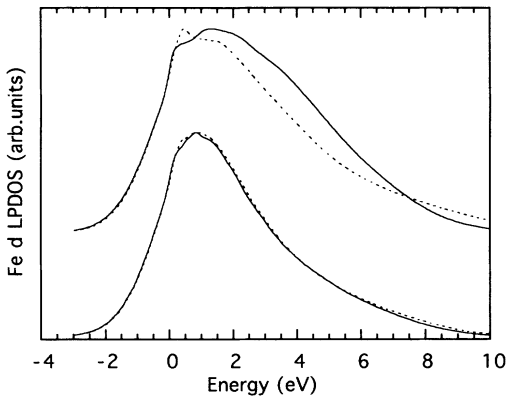

FIG. 11. The influence of a local Fe $2p_{3/2}$ core hole on the SXA spectra of α-$FeSi_2$ (top curves) and β-$FeSi_2$ (bottom curves) is demonstrated. Dashed lines show the results of the band-structure calculation without the presence of the core hole, while the core hole potential was included in the calculations giving rise to the curves drawn by solid lines. In order to compare to the experimental data the LPDOS as shown in Fig. 5 has been cut off at E_F and convoluted with a Gaussian of 1 eV FWHM. The curves have been normalized to their maximum.

Taking this specific shape into account, the influence of the core hole can indeed be described in a simple picture as shifting weight towards lower energies. In this process the peak described above can be pictured as "shifting through E_F" and hence its unoccupied part, giving rise to the shoulder in the SXA spectra, is reduced. Thus moving spectral weight towards lower energies results in an intensity *decrease* close to E_F for the specific shape of the DOS in α-$FeSi_2$. In β-$FeSi_2$, on the other hand, the impact of the core hole on the unoccupied states is not noticeable at the level of the experimental resolution due to the absence of a sharp, isolated feature close to the Fermi level.

We thus conclude that the frequently used simple picture for the impact of the core hole in SXA ("the core hole tends to shift spectral weight down towards E_F") has only limited applicability. In general, the specific shape of the DOS has to be taken into account when discussing the influence of the core hole.

The absorption edge in β-$FeSi_2$ was found to be shifted 0.56 eV towards higher energies as compared to the absorption edge in α-$FeSi_2$. We want to point out that due to the SXA process this shift reflects DOS properties in the presence of a core hole at the Fe site, according to the final state rule. However, the comparison of the band-structure calculations including and neglecting the effect of the core hole shows that the presence of the core hole does not alter the magnitude of the shift between α-$FeSi_2$ and β-$FeSi_2$ significantly (see Fig. 11). We will thus use this value as the shift we expect in the ground state, i.e., without the presence of a core hole.

Though SXE and SXA spectroscopy are performed

in two separate experiments without a common energy scale, it is possible to determine the gap in the Fe d DOS of β-$FeSi_2$ by combining the shifts observed in relation to α-$FeSi_2$ in SXE and SXA. The shift in SXE is -0.24 eV, while a 0.56 eV shift is seen in SXA. These shifts were determined comparing the high-energy cutoffs in SXE and the absorption edges in SXA. From this we determine the overall gap in the symmetry- and site-selected Fe d DOS of β-$FeSi_2$ as 0.8 ± 0.2 eV.

As α-$FeSi_2$ is the common reference in both spectra, a possible binding energy difference of the Fe $2p_{3/2}$ core level in the two phases does not influence this result. The relatively large error reflects the fact that four spectra have to be used to deduce the magnitude of the gap.

As our experiment is sensitive to an indirect band gap as well as to a direct gap, our value for the symmetry- and site-selected band gap is in agreement with our band structure calculation and with the experimental values reported in the literature.[7–14]

E. As-implanted samples

We will now turn our attention to the emission spectrum of the sample in the as-implanted (ai) state shown previously in Fig. 9. The main peak is in its position and asymmetrical shape similar to the α-$FeSi_2$ and β-$FeSi_2$ spectra. The FWHM of the peak is 3.2 eV, indicating a clear narrowing compared to elemental Fe. A closer look at the peak region suggests an only partly resolved double-peak structure at 705.0 and 705.5 eV, coinciding with the observed peaks in the spectra of β-$FeSi_2$ and α-$FeSi_2$ and elemental Fe. Hence the shape of the SXE spectrum of the as-implanted sample could be due to a superposition of the corresponding spectra of the pure phases.

In order to investigate this hypothesis we have tried to model the SXE spectrum of the as-implanted sample by a linear combination of the SXE spectra of α-$FeSi_2$ and β-$FeSi_2$. As can be seen from Fig. 12, every linear combination (line) results in a model spectrum that has too narrow a FWHM to fit the experimental data (circles). It is thus obvious, that the sample in the as-implanted state can not consist of only α-$FeSi_2$ and β-$FeSi_2$. As can be seen in Fig. 13, the data are much better modeled by a superposition of the α-$FeSi_2$ SXE spectrum with the SXE spectrum of Fe metal. The best coefficients for this superposition were determined by a least squares fit. For every superposition, a normalization factor was included as a free parameter to account for the fact that the relative intensities of the spectra are unknown. The best

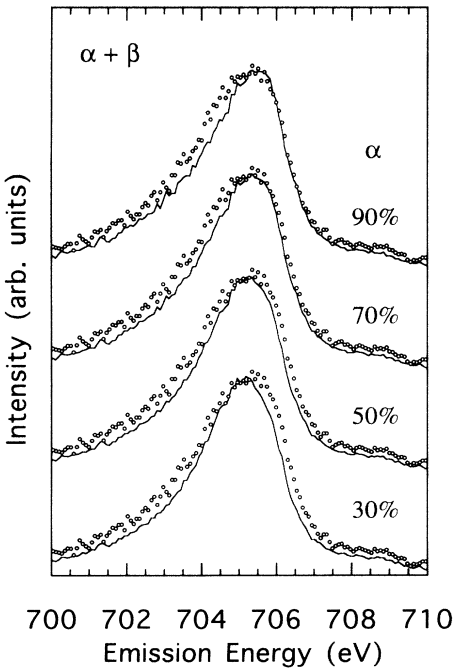

FIG. 12. The SXE spectrum of the IBS sample in an as-implanted state (circles) is compared to a linear superposition of the SXE spectra for α-$FeSi_2$ and β-$FeSi_2$ (lines). The different weight of the α-$FeSi_2$ SXE spectrum in the superposition is indicated to the right. In any superposition, the resulting FWHM is too narrow to simulate the spectrum of the as-implanted sample; thus the sample cannot consist of only α-$FeSi_2$ and β-$FeSi_2$.

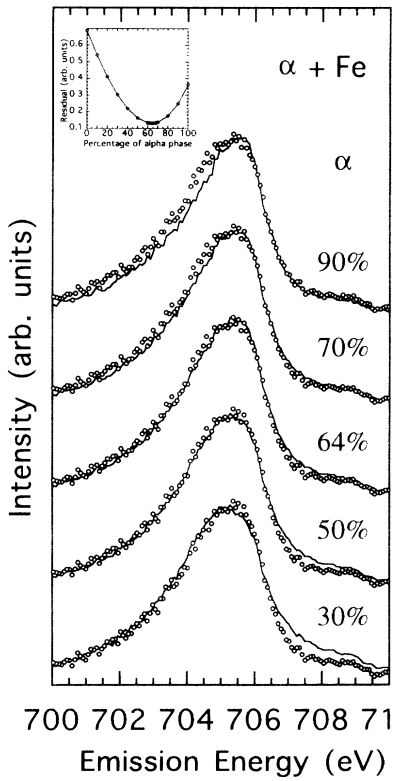

FIG. 13. The SXE spectrum of the IBS sample in an as-implanted state (circles) is compared to a linear superposition of the SXE spectra for α-$FeSi_2$ and elemental Fe (lines). The different weight of the α-$FeSi_2$ SXE spectrum in the superposition is indicated to the right. As indicated in the inset, the best fit to the data is obtained with a superposition consisting of 64% weight on the α-$FeSi_2$ spectrum and 36% weight on the Fe spectrum. The inset shows the residual describing the fit between the experimental spectrum and the superposition as a function of the weight of α-$FeSi_2$ in the superposition.

fit is obtained using a model spectrum consisting of 64% α-$FeSi_2$ and 36% Fe.

Though our data do not permit any quantitative analysis of the composition of the as-implanted sample, they suggest the presence of small amounts of Fe and exclude the possibility that the sample consists of α-$FeSi_2$ and/or β-$FeSi_2$ only. These result are in agreement with recent results obtained in a study of similar samples using electron energy loss spectroscopy, disperisive x-ray analysis, and electron diffraction.[43] Here the as-implanted samples were found to consist mainly of α-$FeSi_2$ with small amounts of β-$FeSi_2$ and excess Fe depending on the preparation conditions.

V. CONCLUSIONS

Using FY-SXA and SXE we were able to investigate the electronic structure in α-$FeSi_2$ and β-$FeSi_2$ layers buried in a Si wafer by means of IBS, demonstrating the capability of these photon-in–photon-out techniques to investigate buried samples *in situ*.

The DOS of d symmetry locally at the Fe sites was determined for the occupied and the unoccupied electronic states. Band-structure calculations for the Fe d DOS of α-$FeSi_2$ and β-$FeSi_2$ were found to accurately predict the spectral features observed for the occupied states. For the α-$FeSi_2$ phase the Fermi level was experimentally found to be located in the high-energy part of the nonbonding, e_g-type Fe d states.

The influence of a Fe $2p_{3/2}$ core hole on the unoccupied states was studied by a supercell calculation. For α-$FeSi_2$ the inclusion of the core hole potential was found to be crucial. The SXE data are in agreement with the final state rule. Due to the specific shape of the α-$FeSi_2$ Fe d DOS, the core hole decreases the relative SXA intensity in the vicinity of the Fermi energy. The β-$FeSi_2$ SXA spectrum is not affected significantly by the core hole.

The formation of the band gap in β-$FeSi_2$ as compared to the metallic α-$FeSi_2$ could be followed in the occupied as well as in the unoccupied electronic states of d symmetry locally around the Fe atoms. From our SXE and SXA experiments, we determine the band gap in the Fe d states of β-$FeSi_2$ as 0.8 ± 0.2 eV. This is in agreement with our calculations which predict a band gap of 0.78 eV.

Correlation in the nonbonding states is exhibited in the presence of double-hole satellites in the SXE spectra, indicating that an extra valence hole is not completely screened out during the core hole lifetime. In the as-implanted state of the IBS process, both α-$FeSi_2$ and Fe were found to be present.

ACKNOWLEDGMENTS

We would like to thank B. Itchkawitz, Z. Xu, and P. D. Johnson for assistance during the X1B work and S. Hulbert for supplying us with an electron gun. We thank G. Remmers and M. Domke for support at the SX-700-II. The authors are indebted to C. Freiburg for his XRD sample characterization and to T. Tiedje for invaluable discussions. One of us (S.E.) is supported by the Deutscher Akademischer Austauschdienst in the HSPII/AUFE program.

*Present address: University of British Columbia, 6224 Agricultural Rd., Vancouver, B.C., Canada V6T 1Z1.

[1] S.P. Murarka and M.C. Peckerar, in *Electronic Materials, Science and Technology*, edited by J. Streichen (Academic, Boston, 1989), p. 267.

[2] S.P. Murarka, *Silicides for VLSI Applications* (Academic, Boston, 1983).

[3] J.C. Hensel, A.F. Levi, R.T. Tung, and J.M. Gibson, Appl. Phys. Lett. **47**, 151 (1985).

[4] Y. Dusausoy, J. Protas, R. Wandji, and B. Roques, Acta Crystallogr. Sec. B **27**, 1209 (1971).

[5] *Pearson's Handbook of Crystallographic Data for Intermetallic Phases*, edited by P. Villars and L.D. Calvert (American Society for Metals, Metals Park, OH, 1985), Vol. 1.

[6] M.E. Schlesinger, Chem. Rev. **90**, 607 (1990).

[7] K. Radermacher, R. Carius, and S. Mantl, Nucl. Instrum. Methods Phys. Res. Sect. B **84**, 163 (1994).

[8] C. Giannini, S. Lagomarsino, F. Scarinci, and P. Castrucci, Phys. Rev. B **45**, 8822 (1992).

[9] K. Lefki and P. Muret, Appl. Surf. Sci. **65/66**, 772 (1993).

[10] M.C. Bost and J.E. Mahan, J. Appl. Phys. **64**, 2034 (1988).

[11] K. Lefki, P. Muret, N. Cherief, and R.C. Cinti, J. Appl. Phys. **69**, 352 (1991).

[12] C.A. Dimitriadis, J.H. Werner, S. Logothetidis, M. Stutzmann, J. Weber, and R. Nesper, J. Appl. Phys. **68**, 1726 (1990).

[13] M. De Crescenzi, G. Gaggiotti, N. Motta, F. Patella, A. Balzarotti, G. Mattogno, and J. Derrien, Surf. Sci. **251/252**, 175 (1991).

[14] W. Raunau, H. Niehus, and G. Comsa, Surf. Sci. Lett. **284**, L375 (1993).

[15] N.E. Christensen, Phys. Rev. B **42**, 7148 (1990).

[16] S. Mantl, Mater. Sci. Rep. **8**, 1 (1992).

[17] K. Radermacher, S. Mantl, Ch. Dieker, and S. Lüth, Appl. Phys. Lett. **59**, 2145 (1991).

[18] S. Mantl, Nucl. Instrum. Methods. Phys. Res. Sect. B **80/81**, 895 (1993).

[19] R. Eppenga, J. Appl. Phys. **68**, 3027 (1990).

[20] U. von Barth and G. Grossmann, Phys. Rev. B **25**, 5150 (1982).

[21] J.-E. Rubensson, H. Feilbach, J. Lauer, T. Böske, S. Eisebitt, and W. Eberhardt (unpublished).

[22] K. Randall, J. Feldhaus, A.M. Bradshaw, W. Eberhardt, Y. Ma, and P.D. Johnson, Rev. Sci. Instrum. **63**, 1367 (1992).

[23] M. Domke, T. Mandel, A. Puschmann, C. Xue, D.A. Shirley, G. Kaindl, H. Petersen, and P. Kuske, Rev. Sci. Instrum. **63**, 80 (1992).

[24] S. Eisebitt, T. Böske, J.-E. Rubensson, and W. Eberhardt, Phys. Rev. B **47**, 14 103 (1993).

[25] L. Hedin and S. Lundqvist, J. Phys. C **4**, 2064 (1971).

[26] E. Wimmer, H. Krakauer, M. Weinert, and A. J. Freeman, Phys. Rev. B **24**, 864 (1981).

[27]J.E. Müller and J.W. Wilkins, Phys. Rev. B **29**, 4331 (1984).
[28]P. Lerch, T. Jarlborg, V. Codazzi, G. Loupias, and A.M. Flank, Phys. Rev. B **45**, 11 481 (1992).
[29]R. Nyholm, N. Mårtensson, A. Lebugle, and U. Axelsson, J. Phys. F **11**, 1727 (1981).
[30]J.J. Jia, T.A. Callcott, W.L. O'Brien, D.Y. Dong, D.R. Mueller, D.L. Ederer, Z. Tan, and J.I. Budnick, Phys. Rev. B **46**, 9446 (1992).
[31]B.T. Thole, D.R. Cowan, G.A. Sawatzky, J. Fink, and J.C. Fuggle, Phys. Rev. B **31**, 6856 (1985).
[32]P. Nozières and C.T. De Dominicis, Phys. Rev. **178**, 1097 (1969).
[33]E. Zaremba and K. Sturm, Phys. Rev. Lett. **66**, 2144 (1991).
[34]S. Eisebitt, T. Böske, J.-E. Rubensson, J. Kojnok, W. Eberhardt, R. Jebasinski, S. Mantl, P. Skytt, J.-H. Guo, N. Wassdahl, J. Nordgren, and K. Holldack, Phys. Rev. B **48**, 5042 (1993).
[35]N. Wassdahl, J-E. Rubensson, G. Bray, P. Glans, P. Bleckert, R. Nyholm, S. Cramm, N. Mårtensson, and J. Nordgren, Phys. Rev. Lett. **64**, 2807 (1990).
[36]J.A. Bearden, Rev. Mod. Phys. **39**, 78 (1967).
[37]J.C. Fuggle and N. Mårtensson, J. Electron Spectrosc. Relat. Phenom. **21**, 275 (1980).
[38]V. Kinsinger, I. Dézsi, P. Steiner, and G. Langouche, J. Phys. Condens. Matter **2**, 4995 (1990).
[39]B. Egert and G. Panzner, Phys. Rev. B **29**, 2091 (1984). It is not evident which phase of $FeSi_2$ was investigated.
[40]F. Sirotti, M. De Santis, and G. Rossi, Phys. Rev. B **48**, 8299 (1993).
[41]P.J.W. Weijs, M.T. Czyżyk, J.F. van Acker, W. Speier, J.B. Goedkoop, H. van Leuken, H.J.M. Hendrix, R.A. de Groot, G. van der Laan, K.H.J. Buschow, G. Wiech, and J.C. Fuggle, Phys. Rev. B **41**, 11 899 (1990).
[42]P.J.W. Weijs, G. Wiech, W. Zahorowski, W. Speier, J.B. Goedkoop, M. Czyzyk, J.F. van Acker, E. van Leuken, R.A. de Groot, G. van der Laan, D.D. Sarma, L. Kumar, K.H.J. Buschow, and J.C. Fuggle, Phys. Scr. **41**, 629 (1990).
[43]G. Crecelius, K. Radermacher, and Ch. Dieker, J. Appl. Phys. **73**, 4848 (1993).
[44]C. J. Bradley and A. P. Cracknell, *The Mathematical Theory of Symmetry in Solids* (Oxford University Press, Oxford, 1972).